Supporting Information

Crystal Phase Reconstruction of Bi-(N-C)/$Bi(OH)_3$-Bi_2O_3 for Selective Cleavage of Lignin C_β-O-4 Bond via Fluidized Electrocatalysis

Jingjing Shi[a], Yanju Lu[b], Feng Long[a], Junming Xu[a,b,], Zupeng Chen[b,*], Jianchun Jiang[a,b]*

[a]Institute of Chemical Industry of Forest Products, Chinese Academy of Forestry; Key Lab. of Biomass Energy and Material, Jiangsu Province; National Engineering Lab. for Biomass Chemical Utilization, Nanjing 210042, China

[b]Jiangsu Co-Innovation Center of Efficient Processing and Utilization of Forest Resources, International Innovation Center for Forest Chemicals and Materials, Nanjing Forestry University, Nanjing 210037, China

[*]Corresponding Authors: Junming Xu (xujunming@icifp.cn), Zupeng Chen (czp@njfu.edu.cn)

Characterization techniques

The surface morphology of the catalyst was observed on a Japanese S-4700 scanning electron microscope (SEM) with a working voltage of 15-20 kV and distance of 3 mm. The micro lattice properties and element spatial distribution of the catalyst were confirmed by TEM, HRTEM, and TEM-EDS spectra, tested with FEI TF0 at an accelerated voltage of 200 kV. The main crystal phases were confirmed by selected area electron diffraction (SAED) patterns. The crystal structure information of the catalyst was confirmed by X-ray diffraction (XRD) on the Rigaku Corporation SmartLab (3 kW) X-ray diffractometer (Japan), with a working voltage of 40 kV, a current of 40 mA, and a radiation source of Cu Kα, λ= 0.154056 nm, with a scanning range and scanning step length of 2θ= 10º- 80º and 0.02º, respectively. The distribution of elemental valence states was tested on the ESCALAB 250XI spectrometer (UK) by Thermo Fisher Scientific for X-ray photoelectron spectroscopy (XPS) using Al Kα (1486.68 eV) monochromatic radiation. Fourier transform infrared spectroscopy (FTIR) was used to detect the metal skeleton bonding structure of the catalysts with a Nicolet 3800 spectrometer (USA). The coordination structure properties of catalysts were measured by Raman spectroscopy using a Renishaw Invia Raman spectrometer (UK), with a laser excitation wavelength of 532 nm. The intrinsic oxygen defects of the catalyst were measured by electron paramagnetic resonance (EPR) using Bruker A300 EPR spectrometer at 100 K. Perform each test with 50 mg of sample and evacuated to vacuum prior to measurement.

Supplementary Figures

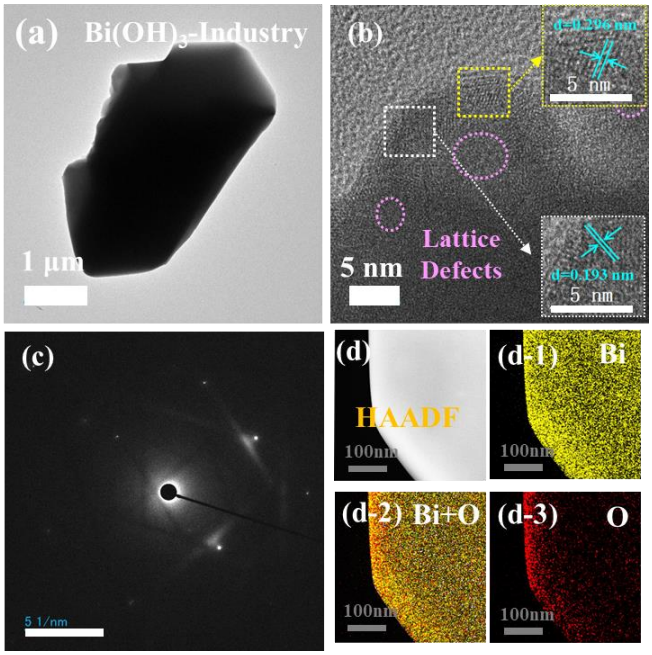

Figure S1. The representative (a) TEM, (b) HRTEM, (c) SAED pattern, and (d) HAADF-STEM images and the corresponding EDS elemental mappings of $Bi(OH)_3$-industry, respectively.

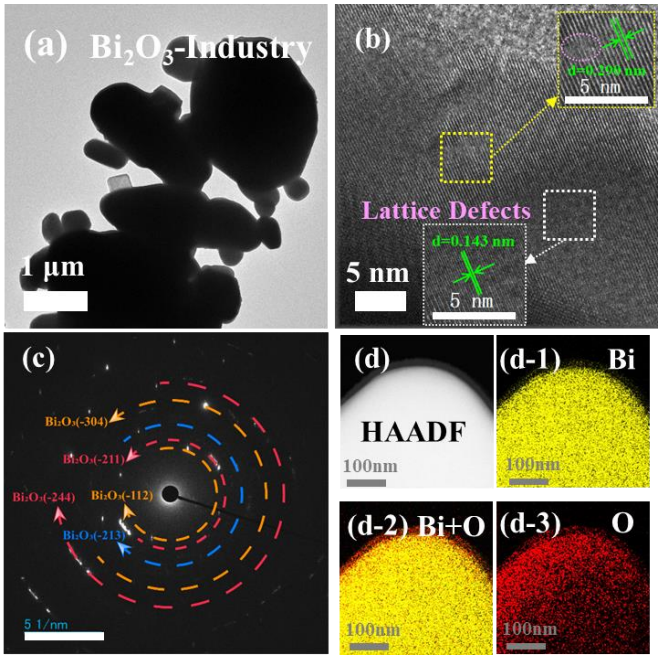

Figure S2. The representative (a) TEM, (b) HRTEM, (c) SAED pattern, and (d) HAADF-STEM images and the corresponding EDS elemental mappings of Bi_2O_3-industry, respectively.

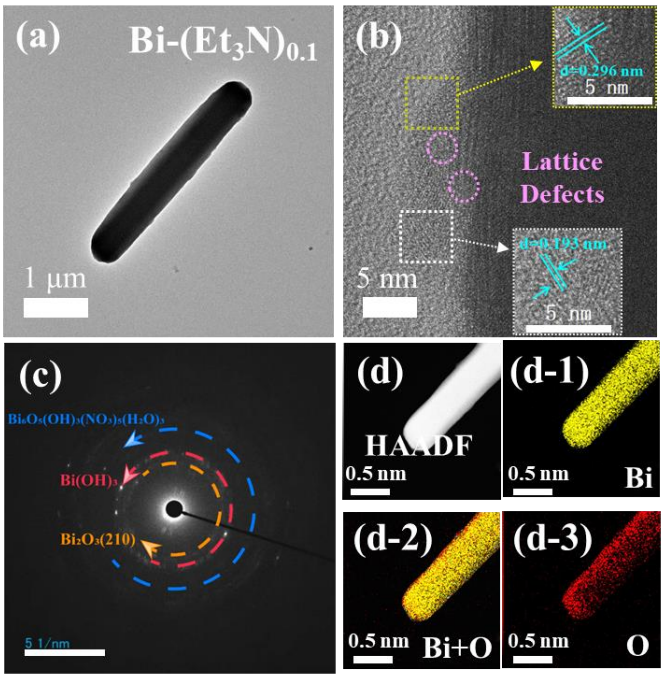

Figure S3. The representative (a) TEM, (b) HRTEM, (c) SAED pattern, and (d) HAADF-STEM images and the corresponding EDS elemental mappings of Bi-$(Et_3N)_{0.1}$, respectively.

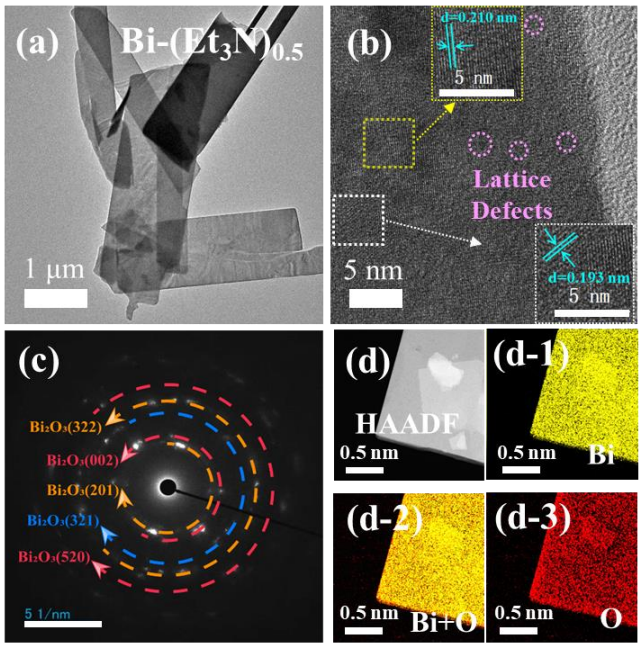

Figure S4. The representative (a) TEM, (b) HRTEM, (c) SAED pattern, and (d) HAADF-STEM images and the corresponding EDS elemental mappings of Bi-$(Et_3N)_{0.5}$, respectively.

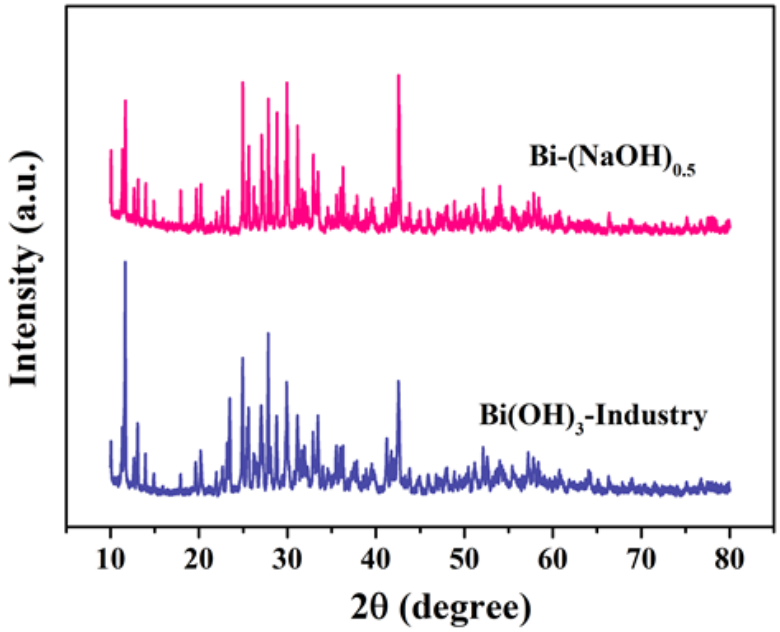

Figure S5. XRD patterns of $Bi(OH)_3$-industry and Bi-$(NaOH)_{0.5}$.

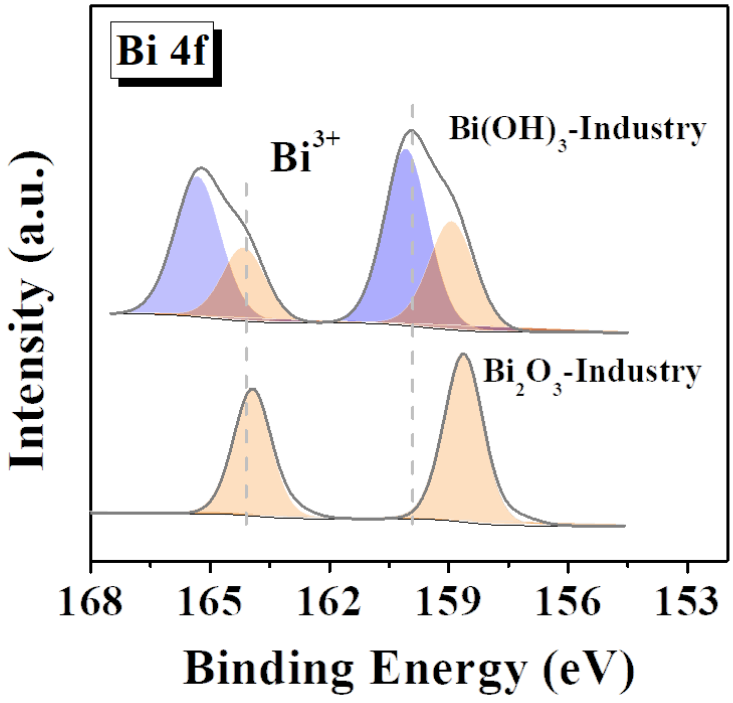

Figure S6. XPS of the Bi 4f energy region of the $Bi(OH)_3$-industry and Bi_2O_3-industry.

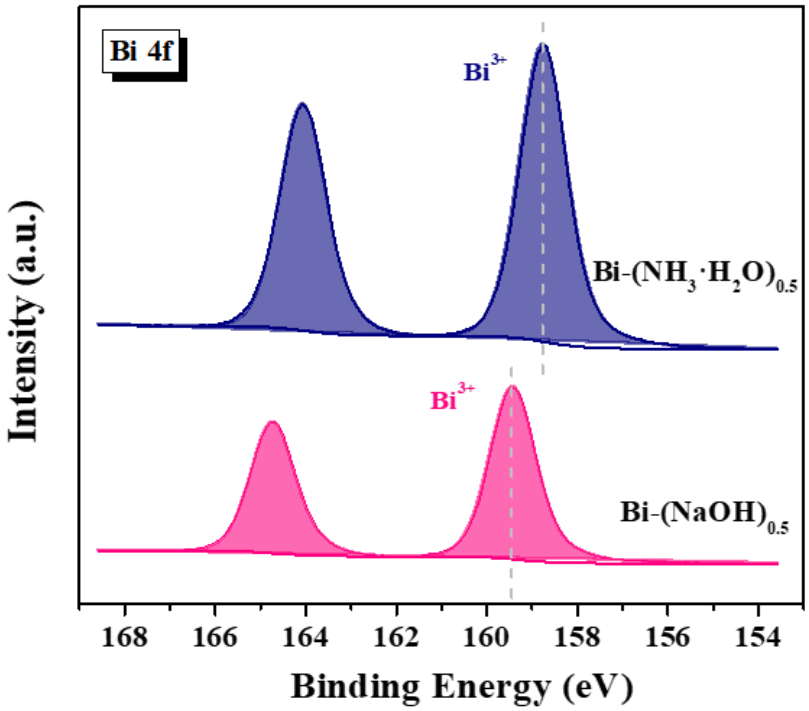

Figure S7. XPS of the Bi 4f energy region of the Bi-$(NaOH)_{0.5}$ and Bi-$(NH_3 \cdot H_2O)_{0.5}$.

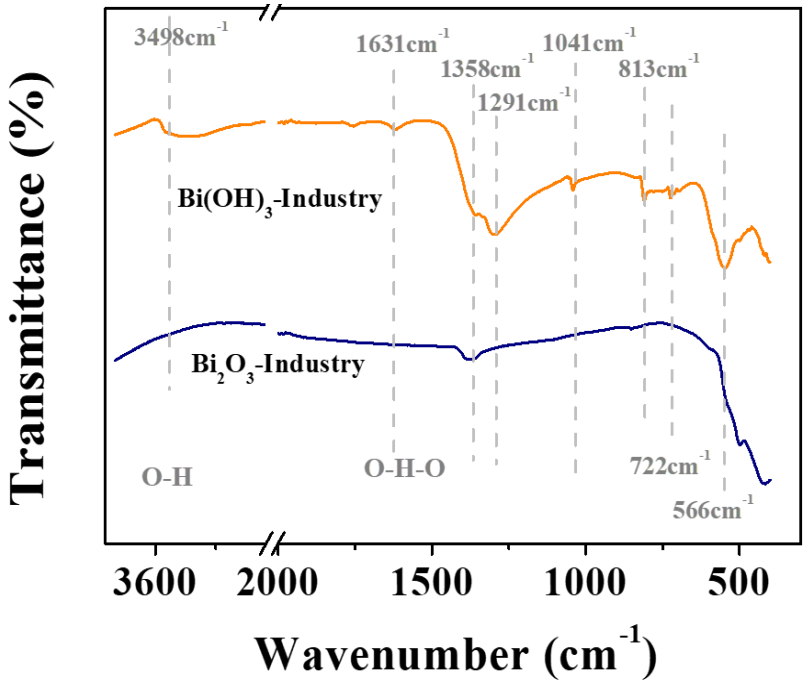

Figure S8. FTIR results of the $Bi(OH)_3$-industry and Bi_2O_3-industry.

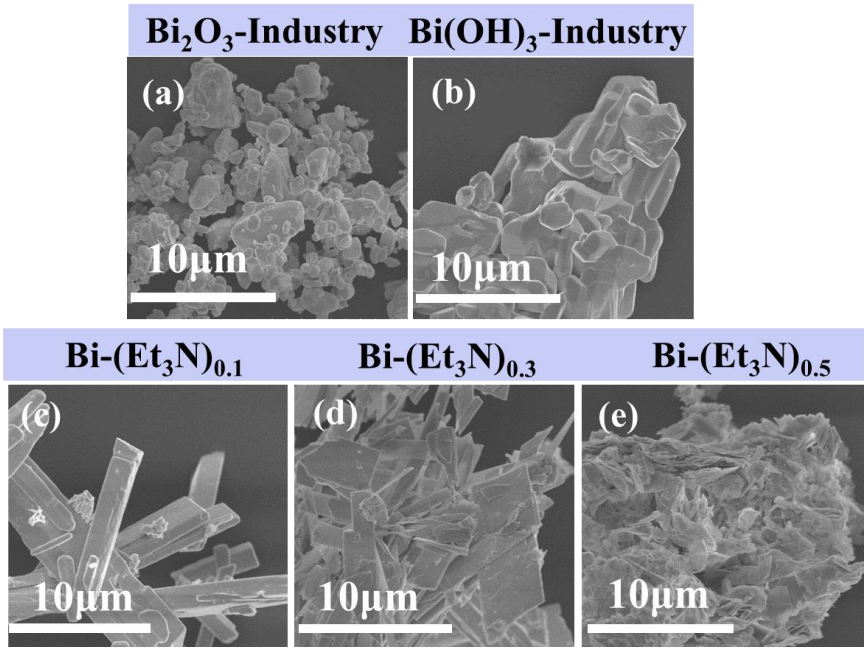

Figure S9. (a) - (e)The SEM patterns of catalysts.

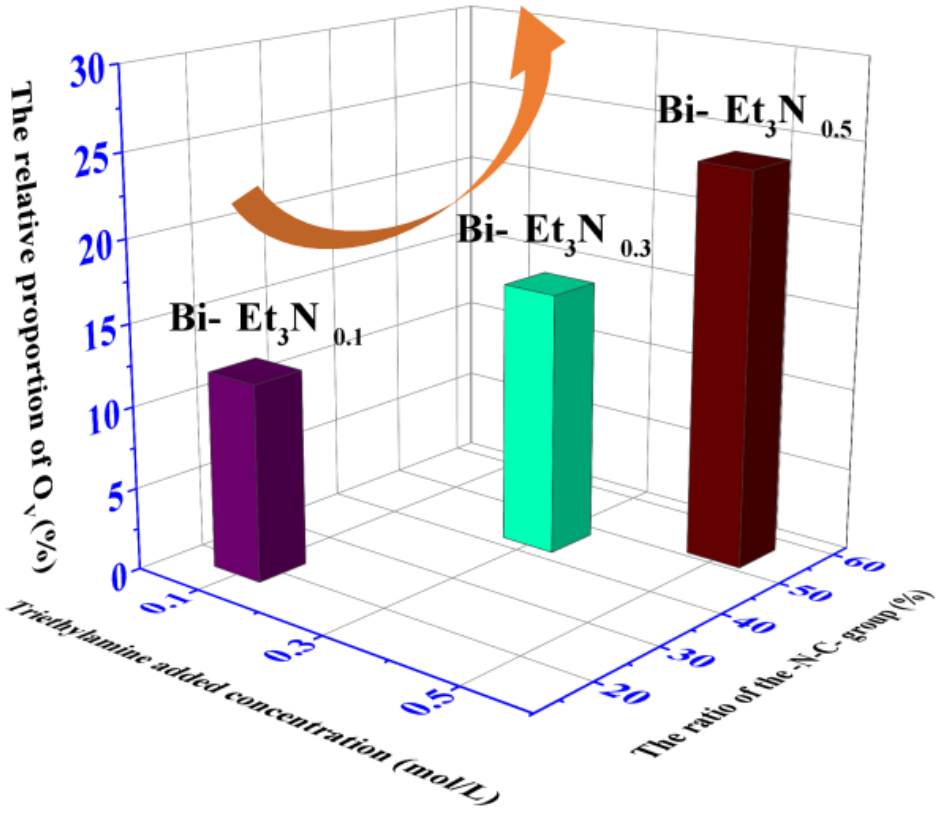

Figure S10. Trend of correlation between triethylamine concentration and the relative content of O_V species and -N-C- groups.

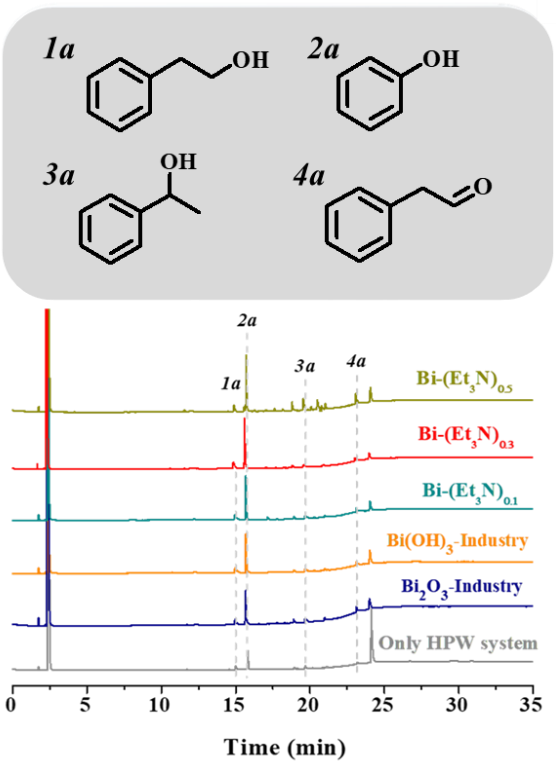

Figure S11. GCMS results of electrochemical reduction experiments of 2-phenoxy-1phenylethanol under different catalysts.

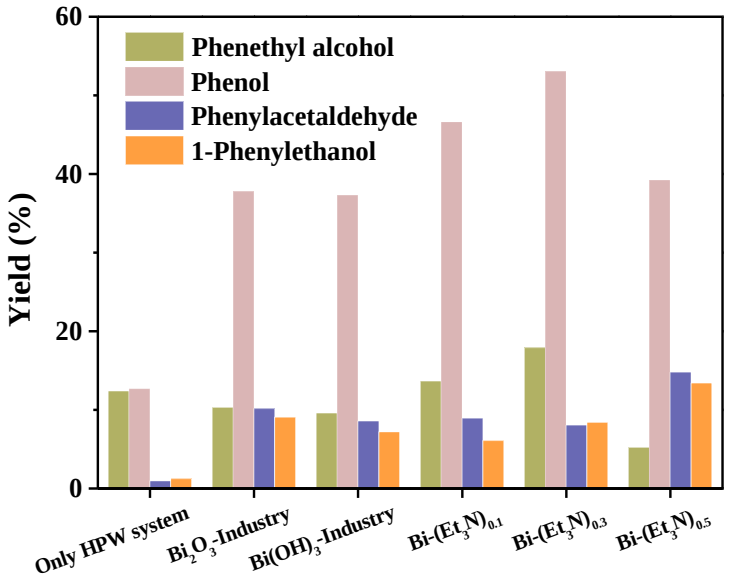

Figure S12. The monomer yields corresponding to different catalysts for the conversion of 2-phenoxy-1-phenylethanol.

(Reaction conditions: 0.02 g catalyst, 30 mM substrate, 60 mA cm^{-2}, 300 rpm, 80 °C, 1.5 h)

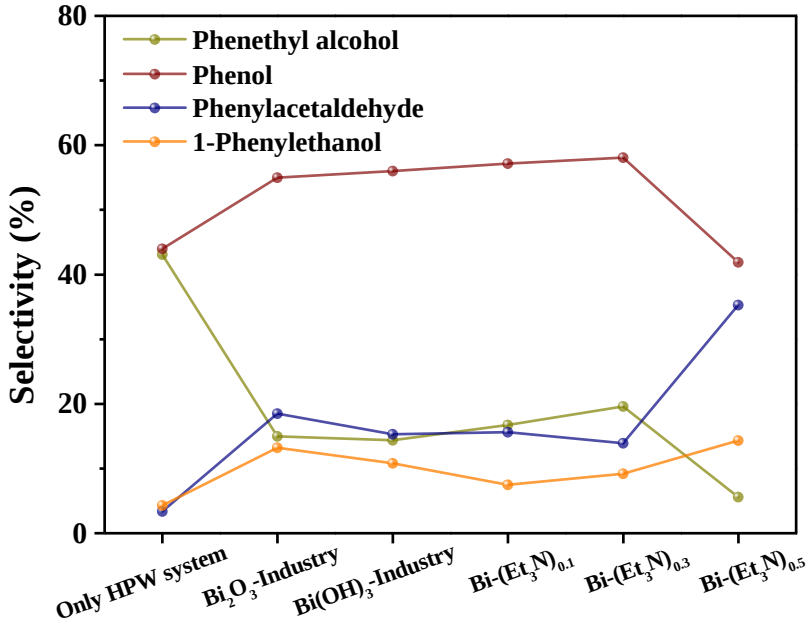

Figure S13. The monomer selectivity corresponding to different catalysts for the conversion of 2-phenoxy-1-phenylethanol.

(Reaction conditions: 0.02 g catalyst, 30 mM substrate, 60 mA cm^{-2}, 300 rpm, 80 °C, 1.5 h)

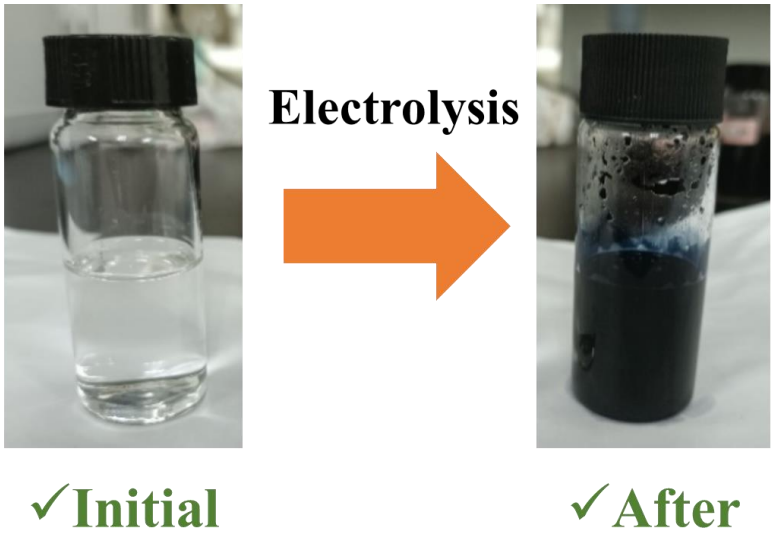

Figure S14. Comparison of state of HPW electrolyte before and after reduction.

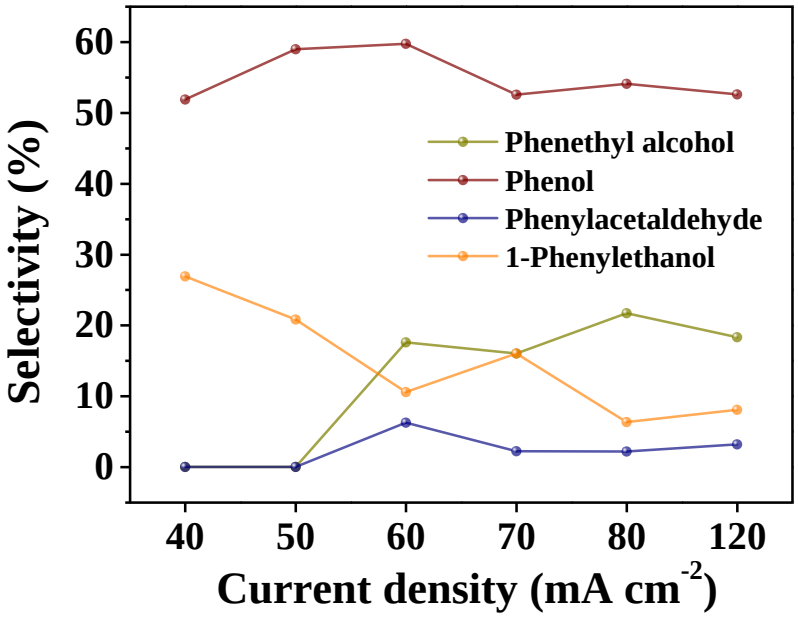

Figure S15. The selectivity of main products at different current densities with Bi-$(Et_3N)_{0.3}$.

(Reaction conditions: 0.02 g Bi-$(Et_3N)_{0.3}$, 30 mM substrate, 300 rpm, 80 °C, 1.5 h)

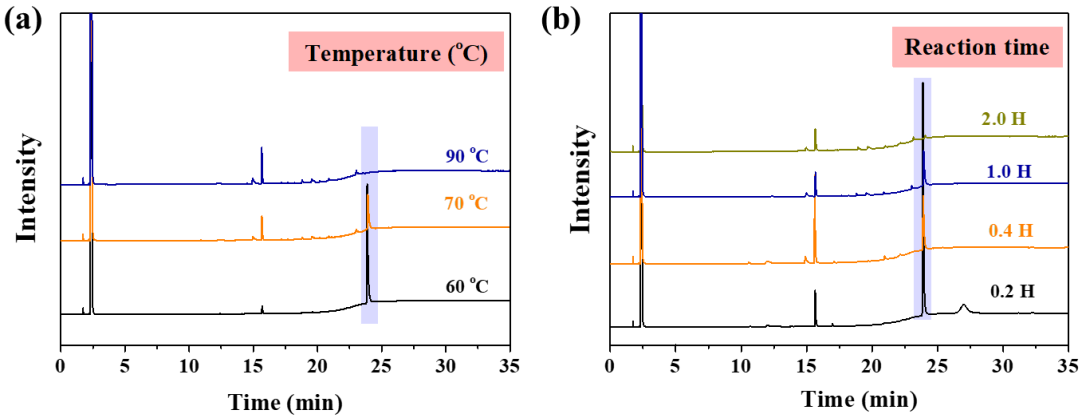

Figure S16. (a), (b) The GCMS results corresponding to 2-phenoxy-1-phenylethanol under different reaction temperatures and times with Bi-$(Et_3N)_{0.3}$.

(Reaction conditions: 0.02 g Bi-$(Et_3N)_{0.3}$, 30 mM substrate, 60 mA cm^{-2}, 300 rpm)

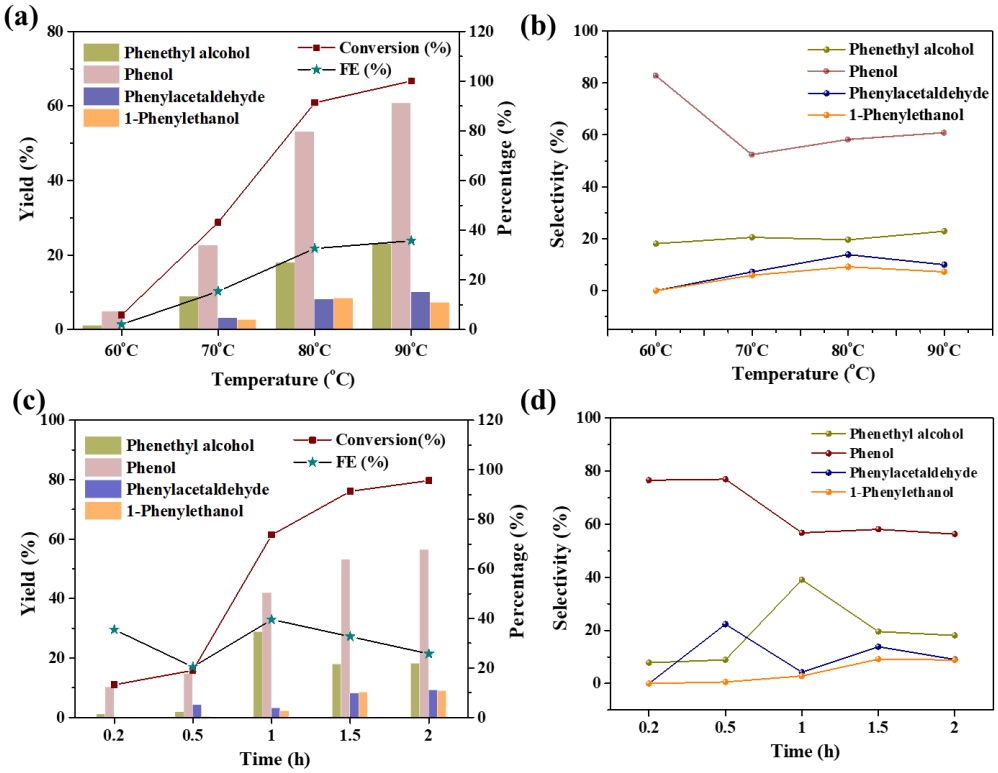

Figure S17. The corresponding conversion (%), FE (%), monomer products yield and selectivity at different reaction temperatures (a), (b) and time (c), (d).

(Reaction conditions: 0.02 g Bi-$(Et_3N)_{0.3}$, 30 mM substrate, 60 mA cm^{-2}, 300 rpm)

The effect of different reaction temperature on the electrocatalytic reduction process was investigated by continuous electrolysis for 1.5 hours in a constant current system of 60 mA·cm^{-2} (Fig. S16 and S17). With the increased reaction temperature, the conversion of 2-phenoxy-1-phenylethanol also showed a continuous increase, achieving the complete conversion and the highest selectivity of phenol monomer (60.68%) at 90 °C. Specifically, when the reaction temperature increased from 60 to 80 °C, the yield of *2a* increased from 4.79 to 53.02%. The effect of different reaction times on the hydrogenation efficiency of 2-phenoxy-1-phenylethanol under a constant current system of 60 mA·cm^{-2} at 80 °C were shown in Fig. S17. When electrolyzed for 1.5 hours, the conversion reached as high as 91.32%. However, with the reaction time increased to 2 hours, the conversion reached 95.68%, but the FE decreased to 25.64%, as too long reaction time would lead to the increase of FE of competitive HER.

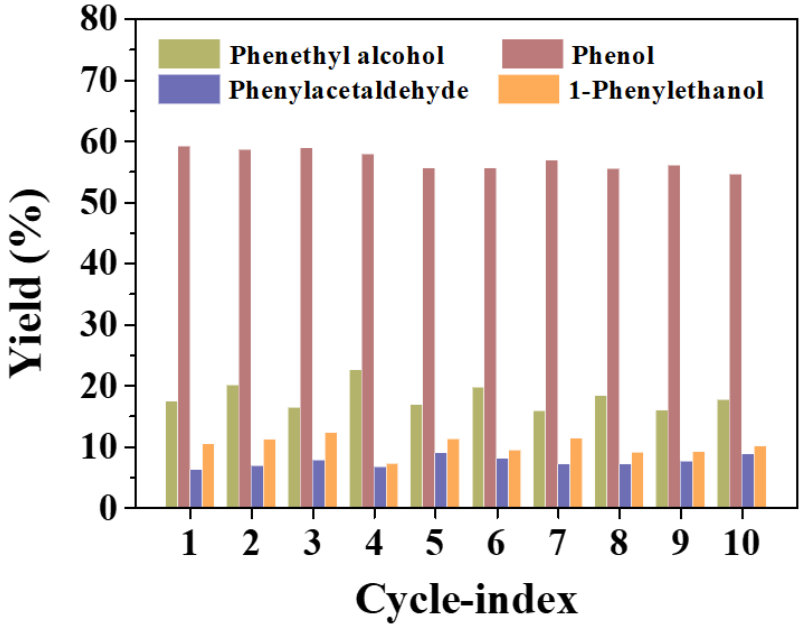

Figure S18. The yield distribution of monomers obtained from 2-phenoxy-1-phenylethanol in 10 consecutive electrolysis cycles under Bi-$(Et_3N)_{0.3}$.

(Reaction conditions: 0.02 g catalyst, 30 mM substrate, 60 mA cm^{-2}, 300 rpm, 90 °C, 1.5 h)

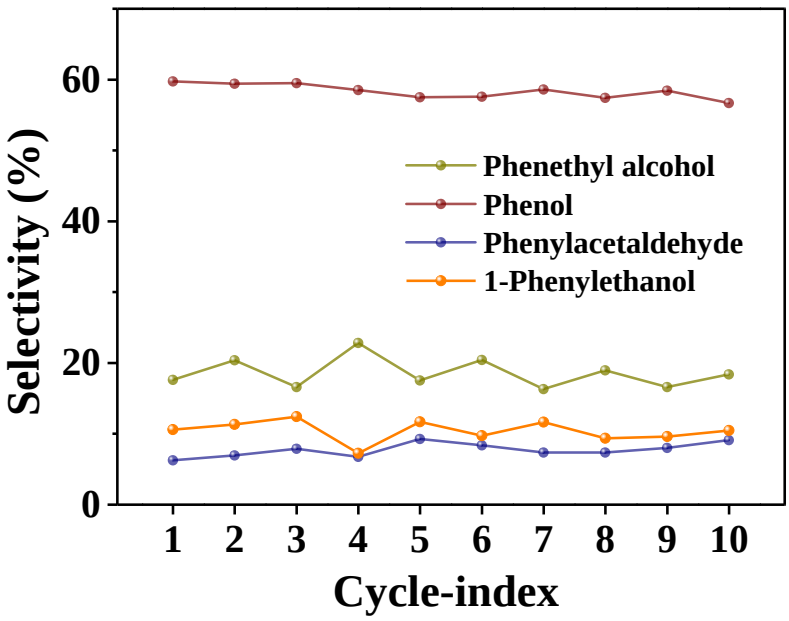

Figure S19. The selectivity of the monomer derived from 2-phenoxy-1-phenylethanol during 10 consecutive electrolysis cycles under the catalysis of Bi.

(Reaction conditions: 0.02 g catalyst, 30 mM substrate, 60 mA cm^{-2}, 300 rpm, 90 °C, 1.5 h)

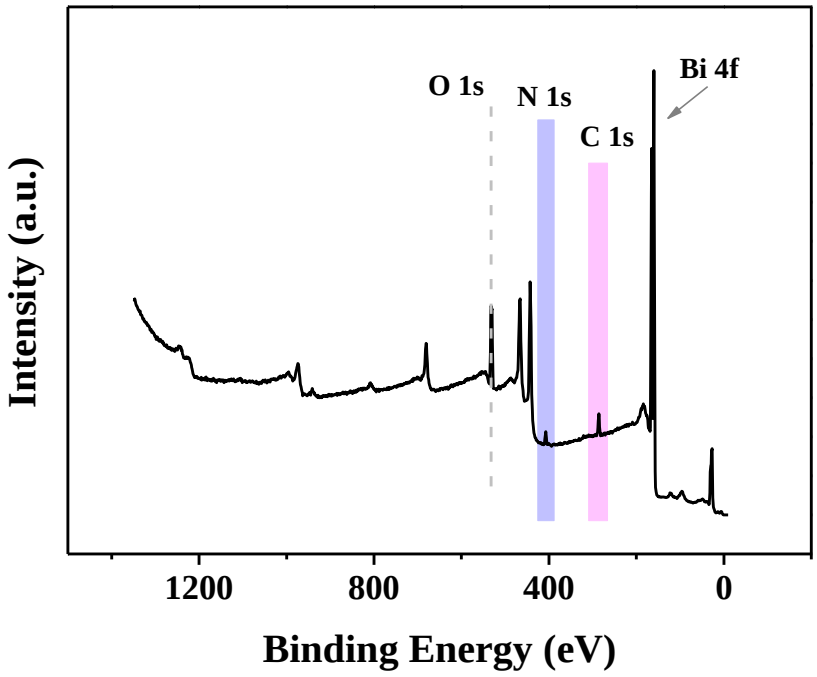

Figure S20. XPS total spectrum of post-reaction Bi-$(Et_3N)_{0.3}$.

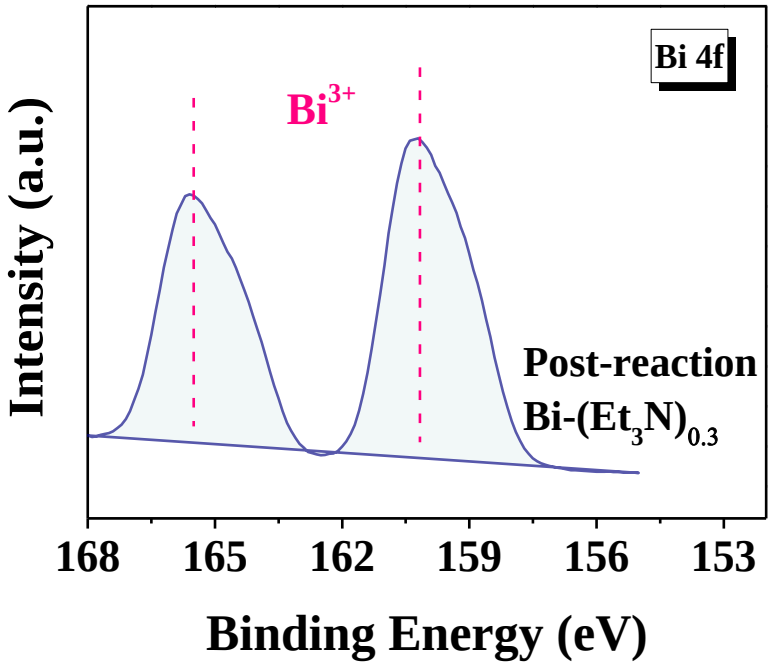

Figure S21. The XPS of Bi 4f energy region of post-reaction Bi-$(Et_3N)_{0.3}$.

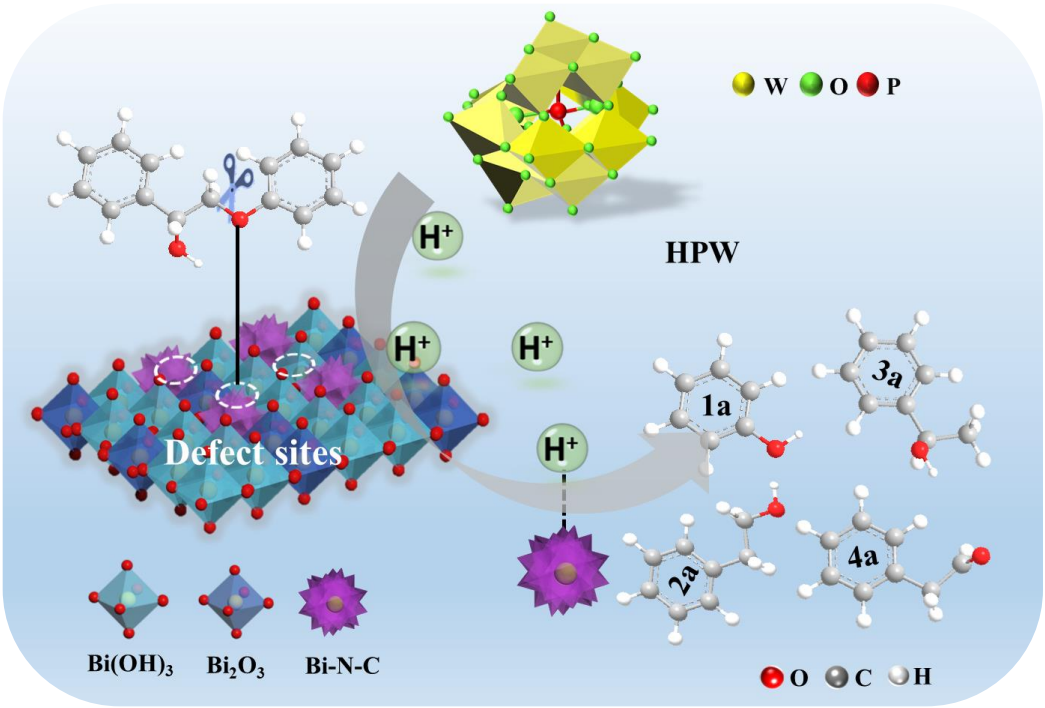

Figure S22. Reaction process of lignin model compounds on Bi-$(Et_3N)_{0.3}$.

Supplementary Tables

Table S1 Comparison of reaction catalysts

Num	Catalyst	Conversion (%)	Yield /Selectivity (%)			
			1a	***2a***	***3a***	***4a***
1	/	28.78	12.39/43.06	12.65/44.98	1.22/4.25	0.96/3.34
2	Bi_2O_3-industry	68.69	10.26/14.94	37.76/54.97	9.05/13.17	10.15/18.46
3	$Bi(OH)_3$-industry	66.61	9.56/14.36	37.31/56.01	7.19/10.79	8.55/15.27
4	Bi-$(Et_3N)_{0.1}$	81.65	13.64/16.70	43.64/57.12	6.07/7.44	8.91/15.59
5	Bi-$(Et_3N)_{0.3}$	91.32	17.88/19.58	53.02/58.06	8.37/9.17	8.05/13.87
6	Bi-$(Et_3N)_{0.5}$	93.74	5.18/5.53	39.24/41.86	13.39/14.28	14.76/35.27

Reaction conditions: 0.05 g catalyst, 30 mM 2-phenoxy-1-phenylethanol, 60 mA cm^{-2}, 80 ℃, 1.5 h, 300 rpm.

Table S2. Comparison of different reaction substrates

Model compound	Structural formula	Conversion (%)
2-phenoxy-1-acetophenone	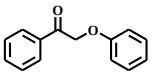	94.87
Phenyl phenylacetate	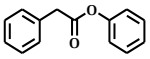	93.11
Phenoxyethylbenzene	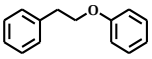	77.25
Benzyl phenyl ether	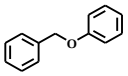	79.24
5-HMF	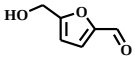	100
2-furoic acid		100
2-methylfuran		100

Table S3. Comparison of different reaction catalysts

Number	Catalyst	Conversion (%)	Yield of phenol (%)	FE (%)
1	$Ni(OH)_2$-industry	55.51	25.10	19.836
2	Ni-$(Et_3N)_{0.3}$	63.29	61.44	22.614
3	Cr-$(Et_3N)_{0.3}$	45.41	18.18	16.224
4	Fe-$(Et_3N)_{0.3}$	60.58	24.99	21.648
5	5% Pt/SiO_2	59.39	29.02	21.222
6	5% Pt/B-GO	77.72	46.74	27.768
7	5% Pt/C-industry	93.37	43.32	33.36